J. Plasma Physics (1998), *vol.* 60, *part* 1, *pp.* 29–48. Printed in the United Kingdom
© 1998 Cambridge University Press

The L mode in electromagnetic proton-cyclotron waves in plasmas modelled by a Lorentzian distribution function

PEDRO VEGA,[1,2] LUIS PALMA[1,2] and RENE ELGUETA[2,3]

[1] Universidad de La Serena, Facultad de Ciencias, Departamento de Física, Casilla 554, La Serena, Chile

[2] Instituto de Investigación Científica de Coquimbo, IICC, Coquimbo, Chile

[3] Universidad Diego Portales, Facultad de Ciencias de la Ingeniería, Santiago, Chile

(Received 10 January 1997 and in revised form 19 August 1997)

The L mode in electromagnetic proton-cyclotron waves (EPCWs) propagating parallel to a uniform ambient magnetic field is studied here analytically. A generalized Lorentzian distribution function is used to model the plasma. Analytical expressions for the wavenumber and for both the temporal and convective growth rates for a multi-ion plasma are obtained within the linear theory. This analytical approach is appropiate for $\beta_{\|} < 1$, which is the ratio of plasma kinetic pressure to magnetic field pressure. The characteristics of the unstable spectrum are found to be independent of high-energy particles. For a plasma composed of electrons plus hot and cold protons, it is shown that the maximum growth rates as functions of cold-proton concentration δ can always decrease, or can increase until δ reaches a certain peak value and decrease thereafter, or can always increase, depending on the thermal anisotropy of the hot protons. This behaviour is similar to that in Maxwellian plasmas. However, for the convective growth rate, the expression for the optimum cold-proton concentration shows a significant dependence on the spectral index κ. Therefore, when cold protons are injected, it is more difficult to obtain optimum amplification in a Lorentzian plasma than in a Maxwellian plasma. It is also shown that the influence of the high-energy tail on the generation and amplification processes of the EPCWs is controlled by thermal anisotropy and cold-ion population. As a consequence of the latter, temporal and convective growth rates can be larger than, equal to or smaller than those of Maxwellian plasmas, depending on the anisotropy of the hot-proton distribution and on the cold-proton concentration.

1. Introduction

The L mode in electromagnetic proton-cyclotron waves (EPCWs) has been extensively studied for several years (Young *et al.* 1981; Roux *et al.* 1982; Gomberoff and Neira 1983; Gendrin *et al.* 1984; Gomberoff and Vega 1987; Vega *et al.* 1992; Anderson *et al.* 1992*a*, *b*). These waves have been widely studied in linear theory, and all theoretical developments have assumed a Maxwellian distribution function for the basic undisturbed state of the plasma (see e.g. Gomberoff and Cuperman 1982; Gomberoff and Neira 1983; Gendrin *et al.* 1984; Gomberoff and Vega 1987;

https://doi.org/10.1017/S0022377898006382 Published online by Cambridge University Press

Vega *et al.* 1992). However, observational studies on natural space plasmas, e.g. planetary magnetospheres, astrophysical plasmas, and the solar wind (Vasyliunas 1968; Williams *et al.* 1988; Lui and Krimigis 1983; Mauk *et al.* 1991; Ogilvie *et al.* 1993), have clearly shown that the particle-velocity distribution exhibits a non-Maxwellian high-energy tail that can best be modelled by a generalized Lorentzian (or kappa) distribution function. This distribution function contains the spectral index κ, representing the relative importance of the high-energy tail of the plasma distribution function. Accordingly, a new special function Z^*_κ has been defined based on the kappa distribution (Summers and Thorne 1991, 1992). Z^*_κ is called the modified plasma dispersion function, and is expected to be instrumental in studying micro-instabilities in multicomponent plasmas for particle distributions having a high-energy tail.

In order to understand the amplification process of EPCWs, several authors have analysed the influence of ion components and thermal anisotropy on the linear growth rate, by means of an analytical approach for a Maxwellian distribution function (see e.g. Gomberoff and Vega 1987, and references therein). In particular, Gomberoff and Vega (1989) analysed the influence of the thermal effects of the ions on the linear growth rate for Maxwellian plasmas. They argue that this approach is appropiate for plasmas with $\beta_\| < 1$, and that it continues to be a good approximation even for large-$\beta_\|$ plasmas ($\beta_\| \approx 1$), provided that the ion components are either not too hot or of a very low density – cases that are common in magnetospheric and other space plasmas.

Xue *et al.* (1993) obtained a general dispersion relation for field-aligned EPCWs by using the modified plasma dispersion function. They presented numerical solutions to the exact governing equation for the wave growth, and compared the growth rate for a bi-Maxwellian distribution with the one for a bi-Lorentzian distribution. They showed that the results are sensitive to the spectral index κ of the kappa distribution, and that the presence of a pronounced high-energy tail allows the electromagnetic proton-cyclotron instability to extend over a much broader frequency range than is expected for a Maxwellian plasma. This study assumed the background plasma to be composed of a single ion species. Xue *et al.* (1993) also pointed out that the frequently used analytical approach mentioned above is too restrictive. Later, Xue *et al.* (1996) studied the growth rate of the L mode in EPCWs under terrestrial magnetospheric conditions; they used an anisotropic kappa particle distribution to model the energetic ring-current ions. By considering a plasma composed of H^+, He^+, and O^+, they showed that convective growth rates can be substantially smaller than the values obtained using a bi-Maxwellian distribution function. Xue *et al.* considered variations in the growth rates in three cases:

(i) by varying the characteristic parameters of anisotropic energetic protons;

(ii) by varying the total ambient plasma density;

(iii) by varying the helium composition.

In order to obtain a good understanding of the EPCWs, it is necessary to obtain analytical expressions for the wavenumber and the growth rate. A detailed analysis of the wave propagation characteristics and the amplification process under space-plasma conditions is possible through these equations. Most space plasmas have more than just one ion species, and each population can consist of a mixture of hot and cold components (Young *et al.* 1981; Christon *et al.* 1989; Ogilvie *et al.* 1993).

https://doi.org/10.1017/S0022377898006382 Published online by Cambridge University Press

Therefore one may expect analytical expressions to show the relationship between each ion population and its characteristic plasma parameters when comparing the dispersive properties and excitation mechanisms for EPCWs in a bi-Maxwellian plasma with those corresponding to a Lorentzian distribution. In this context, satellite observations have shown that ion concentrations and thermal anisotropy for energetic protons can change significantly; for example, the values of A_p range from about 0.2 to about 4 (see e.g. Roux *et al.* 1982; Marsch *et al.* 1982). One may then expect these variations to affect the influence of high-energy particles on EPCWs.

This study will examine the electromagnetic proton-cyclotron instability analytically within the linear theory for plasmas modelled by a kappa distribution function. To this end, the general dispersion relation for the L mode is obtained in Sec. 2; also, the terms corresponding to the hot and cold components respectively are each written separately. Analytical expressions for the wavenumber and for both the temporal and convective growth rates are then obtained as functions of plasma parameters for a multi-ion plasma. The marginal stability condition implies that the marginal mode is similar to that corresponding to a Maxwellian plasma. It is shown here that the characteristics of the unstable frequency spectrum are not influenced by high-energy particles. Space plasma conditions are represented in Sec. 3 by assuming that only two species (protons and electrons) with two proton components (the anisotropic energetic component and the isotropic cold component) are present. A comparison of the analytical results obtained here for the temporal growth rate with those numerically obtained by Xue *et al.* (1993) shows that this analytical approach continues to be a very good approximation for $\beta_{\|} < 1$. On the other hand, the behaviour of both the temporal and convective growth rates as functions of the cold-proton concentration δ, the spectral index κ and the thermal anisotropy is analytically and parametrically studied here. Both maximum growth rates behave in the same way as functions of cold proton concentration δ as in a Maxwellian plasma. However, in the case where the maximum convective growth rate increases until δ reaches a certain optimum value δ_{op} and decreases thereafter, the value of δ_{op} depends significantly on the spectral index κ. It is also shown here that the influence of the high-energy tail on wave growth is strongly dependent on both thermal anisotropy values and cold-proton population. In other words, both growth rates can be larger, equal to or smaller than those for Maxwellian plasmas, depending on the anisotropy of the hot-proton distribution function and on the cold-proton concentration. A brief summary and conclusions of the results are given in Sec. 4.

2. Dispersion relation

In order to model a space plasma system, an infinite homogeneous and magnetized plasma consisting of ions and electrons described by bi-Lorentzian distribution functions of the form (Xue *et al.* 1993)

$$f_\kappa(v_{\|}, v_\perp) = \frac{1}{\pi^{3/2}\Theta_\perp^2\,\Theta_{\|}\kappa^{3/2}}\frac{\Gamma(\kappa+1)}{\Gamma(\kappa+\frac{1}{2})}\left(1+\frac{v_{\|}^2}{\kappa\Theta_{\|}^2}+\frac{v_\perp^2}{\kappa\Theta_\perp^2}\right)^{-(\kappa+1)} \tag{1}$$

is considered here. The expression $\Theta_{\|,\perp}^2 = [(2\kappa-3)/2\kappa](2k_BT_{\|,\perp}/m)$ represents the effective thermal velocities parallel and perpendicular to the magnetic field respectively for $\kappa > \frac{3}{2}$ (Vasyliunas 1968). In the limiting case when $\kappa \to \infty$, this distribution function approaches the Maxwellian form.

https://doi.org/10.1017/S0022377898006382 Published online by Cambridge University Press

Under these conditions, and assuming that the distribution functions for all the components satisfy the Vlasov equation, the dispersion relation within the linear theory for the L mode in electromagnetic ion-cyclotron waves propagating parallel to the external magnetic field is given by

$$k^2c^2 = \omega^2 + \sum_j \omega_{pj}^2 \left\{ A_j - \frac{1}{k\Theta_{\|j}}[(A_j+1)(\Omega_j-\omega)-\Omega_j]\frac{(\kappa_j-1)^{3/2}}{\kappa_j^{1/2}(\kappa_j-\frac{3}{2})} Z^*_{\kappa_j-1}(\xi_j) \right\}, \tag{2}$$

where $\xi_j = [(\kappa_j-1)/\kappa_j]^{1/2}(\omega-\Omega_j)/k\Theta_{\|j}$, $A_j = (T_{\perp j}/T_{\|j}) - 1$ is the thermal anisotropy, $\omega = \omega_r + i\omega_i$, k is the real wavenumber, ω_{pj} and Ω_j are the plasma frequency and the gyrofrequency respectively of species j, κ_j is the spectral index for each species j, and $Z^*_{\kappa_j-1}(\xi_j)$ is the modified plasma dispersion function for each particle population. Equation (2) is equivalent to the one obtained by Summers and Thorne (1991, equation (39)) corresponding to the L-mode wave. This wave mode corresponds to left-hand circularly polarized waves with frequencies below the ion gyrofrequency; the free-energy source is the ion thermal anisotropy. In other words, the effect of the individual particle motion producing the wave–particle resonant interactions is fundamental in predicting this mode. Therefore kinetic theory is necessary to carry out a detailed study on the physics of this kind of wave mode. In (2), the argument of $Z^*_{\kappa_j-1}(\xi_j)$ contains fundamental information about waves and plasma particles for studying the processes of amplification, damping and generation of these waves.

As the space plasma models under consideration have $\beta_\| = 8\pi n k_B T_\|/B_0^2 < 1$ (see e.g. Ishida *et al.* 1987; Isenberg and Hollweg 1983), one may expect large values for the argument of $Z^*_{\kappa-1}(\xi)$; that is, $|\xi| \to \infty$. This leads us to use the asymptotic expression for $Z^*(\xi)$ (Summers and Thorne 1991) in (2):

$$Z^*_\kappa(\xi) = \frac{i\pi^{1/2}\Gamma(\kappa+1)}{\kappa^{\frac{3}{2}}\Gamma(\kappa-\frac{1}{2})}\left(1+\frac{\xi^2}{\kappa}\right)^{-(\kappa+1)} + Y_\kappa(\xi), \tag{3}$$

where

$$Y_\kappa(\xi) = -\frac{2\kappa-1}{2\kappa}\frac{1}{\xi}\left[1+\frac{\kappa}{2\kappa-1}\frac{1}{\xi^2}+\frac{3\kappa^2}{(2\kappa-1)(2\kappa-3)}\frac{1}{\xi^4}+\ldots\right]. \tag{4}$$

The number of terms to be considered in (3) depends on the characteristic parameters of each plasma component. As $|\xi_j|$ decreases, more and more terms in the expansion $\mathrm{Re}[Z^*_\kappa(\xi)]$ must be taken into account. The fact that in typical space plasmas each species can be a mixture of hot and cold components should be considered in the dispersion relation (2), by means of the number of terms in $Z^*_\kappa(\xi)$, (3). Thus, for cold components, only the first term in the expansion of $Y^*_\kappa(\xi)$ should be considered; that is, $Z^*_\kappa(\xi) \sim -[(2\kappa-1)/2\kappa]/\xi$.

By replacing this expression for $Z^*_\kappa(\xi)$ in (2),

$$k^2c^2 = \omega^2 + \sum_j \omega_{pj}^2 \left\{ A_j - \frac{1}{k\Theta_{\|j}}[(A_j+1)(\Omega_j-\omega)-\Omega_j]\frac{(\kappa_j-1)^{3/2}}{\kappa_j^{1/2}(\kappa_j-\frac{3}{2})} Z^*_{\kappa_j-1}(\xi_j) \right\} - \sum_{jc}\omega_{jc}\frac{\omega}{\omega-\Omega_j}. \tag{5}$$

The summation $\sum_{jc}$ is over all the cold components. This summation includes the electrons, given that they are assumed to satisfy $\Omega_e/(2^{1/2}\alpha_e k) \gg 1$, where α_e is

https://doi.org/10.1017/S0022377898006382 Published online by Cambridge University Press

the electron thermal velocity. The last term in (5) is similar to the one obtained when cold components are modelled by a single isotropic Maxwellian distribution (Gomberoff and Vega 1989).

For hot anisotropic components, the asymptotic expression for $Z^*_{\kappa-1}(\xi_j)$ is replaced in (5), by keeping the first two terms in the expansion of $Y^*_{\kappa-1}(\xi_j)$, (4). Then, by assuming $\omega_r \gg \omega_i$ and $k^2c^2/\omega^2 \gg 1$ as well as quasineutrality (see e.g. Gomberoff and Cuperman 1982), the following expresion for the dispersion relation is obtained from the real part of (5):

$$\frac{k^2c^2}{\omega^2_{pph}} = x^2 \left[\sum_j \frac{z_j(\eta_{jc} + \eta_{jh})M_j}{(1 - M_j x)} \right] \Big/ I(x), \tag{6}$$

where

$$I(x) = 1 + \sum_{jh} \frac{\beta_{\|jh}}{2} \frac{A_j(1 - M_j x) - M_j x}{(1 - M_j x)^3}, \tag{7}$$

and $x = \omega_r/\Omega_p$, $\eta_{jc,h} = (M_j/z_j)(\omega^2_{pjc,h}/\omega^2_{pph})$, $M_j = m_j/z_j m_p$, and z_j is the ion charge. Indices c and h stand for the cold and the hot ion components respectively. In (6) and (7), the summation over j includes all the ions, and the summation over jh includes all the hot-ion components.

It is interesting to note that the dispersion relation (6) is κ-independent, and similar to the one obtained for a Maxwellian plasma (Gomberoff and Vega 1989); it is called the 'corrected semicold approximation'. This result shows that for a plasma characterized by $\beta < 1$, the high-energy tail population does not affect the wave propagation properties of the EPCWs. Therefore the Maxwellian and the Lorentzian plasmas present unstable frequency spectra with identical characteristics. If the third term in the expansion $Y_\kappa(\xi)$ is now included then the dispersion relation becomes κ-dependent. On replacing $\kappa = 2$, which is the value of κ corresponding to the largest proportion of high-energy particles, the only effect, as compared with the equivalent third term in the expansion for a Maxwellian plasma, is a change of sign. Moreover, it is important to point out here that when the plasma is multicomponent, resonances producing cutoffs in the phase velocity occur at $M_j x = 1$. This leads to stop-bands where waves do not propagate.

In order to study the effect of the high-energy tail components on wave growth, analytical expressions for both the temporal and convective growth rate will be obtained below.

2.1. Temporal growth rate

The temporal growth rate is determined from the imaginary part of (5) and is given by

$$\begin{aligned}\gamma_\kappa = {} & \sum_{jh} \left(\frac{\pi}{\beta_{\|jh}} \right)^{1/2} \left(\frac{\eta_{jh} z_j}{M_j} \right)^{3/2} \\ & \times \frac{\Gamma(\kappa_j)[A_j(1 - M_j x) - M_j x]}{(\kappa_j - \frac{3}{2})^{3/2}\Gamma(\kappa_j - \frac{3}{2})} \left[1 + \frac{\eta_{jh} z_j (1 - M_j x)^2}{M_j \beta_{\|jh}(\kappa_j - \frac{3}{2})} \Big/ \frac{k^2c^2}{\omega^2_{pph}} \right]^{-\kappa_j} \\ & \times \left\{ \frac{kc}{\omega_{pph}} \left[\sum_j \frac{z_j(\eta_{jh} + \eta_{jc}) M_j x (2 - M_j x)}{(1 - M_j x)^2} - \frac{k^2c^2}{\omega^2_{pph}} \sum_{jh} \frac{\beta_{\|jh}}{2} M_j F_j(x) \right] \right\}^{-1}, \end{aligned} \tag{8}$$

https://doi.org/10.1017/S0022377898006382 Published online by Cambridge University Press

where

$$F_j(x) = \frac{2[A_j(1 - M_j x) - M_j x] - 1}{(1 - M_j x)^4}.$$

In (8), $\gamma_\kappa = \omega_i/\Omega_p$, κ_j is the spectral index of species j, and Γ is the Gamma function. It is possible to see from (8) that γ_κ is a function of the spectral index κ. This dependence comes from the imaginary part of the modified plasma dispersion function $Z^*_\kappa(\xi)$. The denominator of (8) is identical to the denominator in the Maxwellian case. Also, in the linear theory, the combined effect of the j-ion-cyclotron instabilities is a linear superposition of the j effects; that is, $\gamma_\kappa = \sum_j \gamma_{\kappa_j}$. Thus, by setting $\gamma_{\kappa_j} = 0$ in (8), a frequency that is a marginal mode for the j-ion-cyclotron instability is obtained, i.e. a frequency such that when $x = x_{M_j}$, the j term in (8) becomes zero, and x_{M_j} is given by $A_j/[M_j(A_j + 1)]$. This result is similar to the one obtained in a Maxwellian plasma (Gomberoff and Vega 1987).

2.2. Convective growth rate

The convective growth rate is defined as $S_\kappa = \gamma_\kappa/v_g$, where v_g is the group velocity. By calculating v_g from (6), and by combining it with (8),

$$S_\kappa = \sum_{jh} \frac{\pi^{1/2}}{2\alpha_{\|jh}} \frac{\eta_{jh} z_j}{M_j^2} \times \frac{\Gamma(\kappa_j)[A_j(1 - M_j x) - M_j x]}{(\kappa_j - \frac{3}{2})^{1/2}\Gamma(\kappa_j - \frac{3}{2})} \left[1 + \frac{\eta_{jh} z_j}{M_j \beta_{\|jh}} \frac{(1 - M_j x)^2}{(\kappa_j - \frac{3}{2})} \Big/ \frac{k^2 c^2}{\omega_{pph}^2}\right]^{-\kappa_j} \times \left\{ x^2 \left[\sum_j \frac{z_j(\eta_{jc} + \eta_{jh}) M_j}{(1 - M_j x)} \right] \right\}^{-1}, \tag{9}$$

where $\alpha_{\|jh}$ is the thermal speed of the hot species j parallel to the ambient magnetic field. Equation (9) clearly shows, like (8), that the wave growth is a function strongly dependent on plasma parameters. Therefore it is very important to study this dependence in a Lorentzian plasma and compare it with the dependence in a Maxwellian plasma. In particular, one may expect large differences between S_κ and S_m for smaller values of κ. However, one may also expect these differences to be dependent on the different plasma parameters.

3. Proton-cyclotron instability

Satellite observations have shown a close association between the occurrence of intense ion-cyclotron waves below the proton gyrofrequency and the presence of energetic ($E \approx 20$–100 keV) and anisotropic protons (Roux *et al.* 1982; Gendrin *et al.* 1984). It is well established that these protons provide the free-energy source for the ion-cyclotron instability. In this case, the instability is called the proton-cyclotron instability.

Therefore let us now consider a plasma consisting of only energetic anisotropic protons and a cold-proton component. Under this assumption, the wavenumber k,

https://doi.org/10.1017/S0022377898006382 Published online by Cambridge University Press

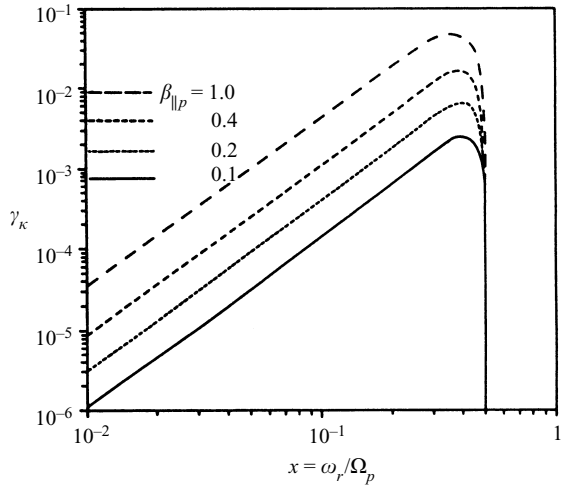


Figure 1. Normalized Lorentzian temporal growth rate versus normalized frequency for $A_p = 1$ and $\kappa = 2$, and several values of $\beta_{\|p}$ (0.1, 0.2, 0.4, and 1.0).

(6), is now given by

$$\frac{k^2c^2}{\omega_{pph}^2} = x^2\frac{1+\delta}{1-x}\Bigg/\left\{1+\frac{\beta_{\|p}}{2}\frac{[A_p(1-x)-x]}{(1-x)^3}\right\}, \tag{10}$$

where $\delta = \eta_{jc}$ is the cold-proton concentration.

The temporal growth rate (8) reduces to

$$\gamma_\kappa = \left(\frac{\pi}{\beta_{\|p}}\right)^{1/2}\frac{\Gamma(\kappa)[A_p(1-x)-x]}{(\kappa-\frac{3}{2})^{3/2}\Gamma(\kappa-\frac{3}{2})}\left[1+\frac{(1-x)^2}{\beta_{\|p}(\kappa-\frac{3}{2})}\Bigg/\frac{k^2c^2}{\omega_{pph}^2}\right]^{-\kappa} \times\left\{\frac{kc}{\omega_{pph}}\left[\frac{x(1+\delta)(2-x)}{(1-x)^2}-\frac{k^2c^2}{\omega_{pph}^2}\frac{\beta_{\|p}}{2}\frac{2[A_p(1-x)-x]-1}{(1-x)^4}\right]\right\}^{-1}, \tag{11}$$

and the convective growth rate (9) can be written as

$$S_\kappa = \frac{\pi^{1/2}}{2\alpha_{\|p}}\frac{\Gamma(\kappa)[A_p(1-x)-x]}{(\kappa-\frac{3}{2})^{1/2}\Gamma(\kappa-\frac{3}{2})}\left[1+\frac{(1-x)^2}{\beta_{\|p}(\kappa-\frac{3}{2})}\Bigg/\frac{k^2c^2}{\omega_{pph}^2}\right]^{-\kappa}\left(x^2\frac{1+\delta}{1-x}\right)^{-1}. \tag{12}$$

3.1. Semicold approximation

An analytical study of how the influence of the high-energy tail population on wave growth is affected by other plasma parameters is presented below. To this end, the semicold approximation is considered; that is, the denominator in (10) is taken as 1, and the temporal growth rate (11) becomes

$$\gamma_\kappa = \left(\frac{\pi}{\beta_{\|p}}\right)^{1/2}\frac{\Gamma(\kappa)[A_p(1-x)-x]}{(\kappa-\frac{3}{2})^{3/2}\Gamma(\kappa-\frac{3}{2})}\left[1+\frac{(1-x)^2}{\beta_{\|p}(\kappa-\frac{3}{2})}\Bigg/\left(x^2\frac{1+\delta}{1-x}\right)\right]^{-\kappa} \times\left[x^2\left(\frac{1+\delta}{1-x}\right)^{1/2}\frac{(1+\delta)(2-x)}{(1-x)^2}\right]^{-1}. \tag{13}$$

https://doi.org/10.1017/S0022377898006382 Published online by Cambridge University Press

3.1.1. Validity of the approach. In order to assess the validity of the semicold approximation, our results are compared with those obtained by Xue *et al.* (1993). Thus, Fig. 1 shows the temporal growth rate γ_κ as a function of $x = \omega_r/\Omega_p$, for $A_p = 1$, $\delta = 0$ and $\kappa = 2$; the value of κ corresponds to the largest proportion of high-energy particles. Since the values of the $\beta_{\|p}$ were chosen as 0.1, 0.2, 0.4 and 1.0, our approach is expected to be appropriate for $\beta_{\|p} < 1$. It must be said here that many space plasmas have values of $\beta_{\|p}$ of this order (see e.g. Ishida *et al.* 1987; Isenberg and Hollweg 1983; Marsch *et al.* 1982). The agreement between our results and Fig. 7 in Xue *et al.* (1993) is very good, especially for small values of $\beta_{\|p}$, i.e. 0.1, 0.2 and 0.4. When $\beta_{\|p} = 1.0$, our semicold approximation deviates from the results obtained numerically by Xue *et al.* (1993). The temporal growth rate obtained here is larger than theirs. However, these deviations can be corrected by adding more terms to $\mathrm{Re}[Z^*_\kappa(\xi_p)]$, (4). In fact, when $\beta_{\|p}$ approaches 1, the argument of the modified plasma dispersion function (Summers and Thorne 1991) approaches 1 as well. So, more and more terms in the expansion $\mathrm{Re}[Z^*_\kappa(\xi_p)]$ must be considered. In any case, for the study of wave growth, the relative behaviour of γ_κ as a function of plasma parameters is more relevant than its exact value when the deviation of our approach is small. Moreover, when unstable modes get closer to the proton gyrofrequency, it is possible to see that the wavenumber k becomes larger and larger. Thus there is always a frequency band $\Delta\omega = \mid \omega - \Omega_p \mid$ around which the approximation $\xi_p^2 > 1$ no longer holds. Therefore the approximation is good when the width of this frequency band is small compared with the width of the unstable spectrum. As mentioned above, the approximation is good for $\beta < 1$, and becomes better and better as β decreases (Gomberoff and Vega 1989).

3.1.2. Maximum temporal growth rate. Our semicold approximation allows us to obtain enough information about the behaviour of the wave growth as a function of plasma parameters. Thus, for instance, the convective growth rate (12) and the temporal growth rate (13) are both increasing functions of δ up to a certain optimum value δ_{op}, and decrease thereafter. Furthermore, it is possible to see that both growth rates increase for increasing values of A_p, and that the marginal mode for the proton-cyclotron instability is given by $x_m = A_p/(A_p + 1)$.

In particular, δ_{op} can be obtained by equating to zero the first derivative of the growth rate with respect to δ. The application of this procedure to the temporal case leads to the condition

$$Q = \frac{(1-x)^3}{\beta_{\|p} x^2 (1+\delta)} = \frac{3}{2}. \tag{14}$$

This equation shows that the optimum value of δ is a function of the mode x. Therefore the mode that makes γ_κ a maximum should now be calculated in order to obtain the maximum temporal growth rate. This is done by equating to zero the first derivative of γ_κ with respect to x, obtaining

$$\frac{-(A_p+1)}{A_p(1-x)-x} + \frac{1}{2(1-x)}\left(\frac{6Q\kappa}{Q+\kappa-\frac{3}{2}} - 5\right) + \frac{2}{x}\left(\frac{Q\kappa}{Q+\kappa-\frac{3}{2}} - 1\right) + \frac{1}{2-x} = 0. \tag{15}$$

Even though this equation depends on the spectral index κ, when combined with

https://doi.org/10.1017/S0022377898006382 Published online by Cambridge University Press

(14) it gives

$$(A_p + 1)x^3 + (1 - A_p)x^2 - 2(A_p + 2)x + 2A_p = 0. \tag{16}$$

This cubic equation in x depends only on A_p, and gives the mode x_1 that makes the temporal Lorentzian growth rate a maximum. By replacing this value in (14), one obtains the optimum ion concentration $\delta_{\rm op}$ at which γ_κ reaches its maximum value as a function of δ:

$$\delta_{\rm op} = \frac{2(1 - x_1)^3}{3\beta_{\|p} x_1^2} - 1. \tag{17}$$

It is possible to see that (14) and (16) are identical to those corresponding to the Maxwellian case (Gomberoff and Cuperman 1982). Consequently, the optimum value $\delta_{\rm op}$, (17), is similar to the one in the Maxwellian plasma.

The maximum temporal growth rate for x_1 is given by

$$\gamma_{\kappa,\max} = \left(\frac{27\pi}{8}\right)^{1/2} \frac{\beta_{\|p}\Gamma(\kappa)x_1[A_p(1 - x_1) - x_1]}{(\kappa - \frac{3}{2})^{3/2}\Gamma(\kappa - \frac{3}{2})(1 - x_1)^2(2 - x_1)} \left(1 + \frac{3}{2\kappa - 3}\right)^{-\kappa}. \tag{18}$$

Equation (18) shows that the maximum temporal growth rate is a function of the index κ, so differences with respect to the Maxwellian case should be expected.

Figure 2 shows the temporal growth rate γ_κ as a function of $x = \omega_r/\Omega_p$ for $\beta_{\|p} = 0.1$, $\kappa = 2$, and for different values of δ. Each part corresponds to a given value of A_p. Thus, for $A_p = 3$, it follows from (17) that $\delta_{\rm op}$ is negative, meaning that $\gamma_{\kappa,\max}$ should be a monotonically decreasing function of δ. Figure 2(a) illustrates this situation, showing that $\gamma_{\kappa,\max}$ is a clearly decreasing function of δ.

In order to see what happens if A_p is reduced, let us now consider $A_p = 2$. It follows from (17) that $\delta_{\rm op} = 1.75$; and it is seen from (16) that $\gamma_{\kappa,\max}(\delta = \delta_{\rm op})$ should occur at $x_1 = 0.52$. Therefore $\gamma_{\kappa,\max}$ should increase with δ up to $\delta_{\rm op}$, and decrease thereafter. As shown in Fig. 2(b), the expected behaviour is attained, and $\gamma_{\kappa,\max}$ continues to be a very rapidly varying function of δ.

Let us now consider $A_p = 1.0$. From (17), $\delta_{\rm op} = 14.42$, and $\gamma_{\kappa,\max}(\delta = \delta_{\rm op})$ occurs at $x_1 \approx 0.35$. Figure 2(c) illustrates this situation, showing that $\gamma_{\kappa,\max}$ is a sharply varying function of δ. For example, $\gamma_{\kappa,\max}$ exhibits a large increase when the cold-proton concentration increases from $\delta = 0$ to $\delta = \delta_{\rm op}$; for larger increases in δ, $\gamma_{\kappa,\max}$ decreases rapidly.

It is important to note that there is a general decrease of $\gamma_{\kappa,\max}$ when A_p decreases. This is due to the fact that $\gamma_{\kappa,\max}$ is proportional to A_p, as follows from (18). On the other hand, for any given value of A_p, $\gamma_{\kappa,\max}$ shows a significant variation – either as an increasing or as a decreasing function of δ, or as both.

In order to study the deviations from the case of a Maxwellian plasma, the temporal growth rate for the Maxwellian case γ_M is plotted in Fig. 3 as a function of x. The plasma parameters are the same as in Fig. 2. Thus, by comparing Figs 2 and 3, it is possible to see that the behaviour of $\gamma_{\max}$ as a function of δ is very similar in both cases. This behaviour is predictable from (18) and from the corresponding equation for a Maxwellian plasma (see e.g. Gomberoff and Vega 1989), where $\gamma_{\kappa,\max}$ is proportional to A_p in the same way as $\gamma_{M,\max}$. For $A_p = 2$ or 3, $\gamma_{\kappa,\max}$ is always less than $\gamma_{M,\max}$ for any value of δ. However, for $A_p = 1$, the above behaviour occurs only for $\delta > 10$, since for $\delta = 0$ or 1, $\gamma_{\kappa,\max}$ is larger than $\gamma_{M,\max}$. It should be noted that for $\delta = 0$, $\gamma_{M,\max} < 10^{-3}$.

https://doi.org/10.1017/S0022377898006382 Published online by Cambridge University Press

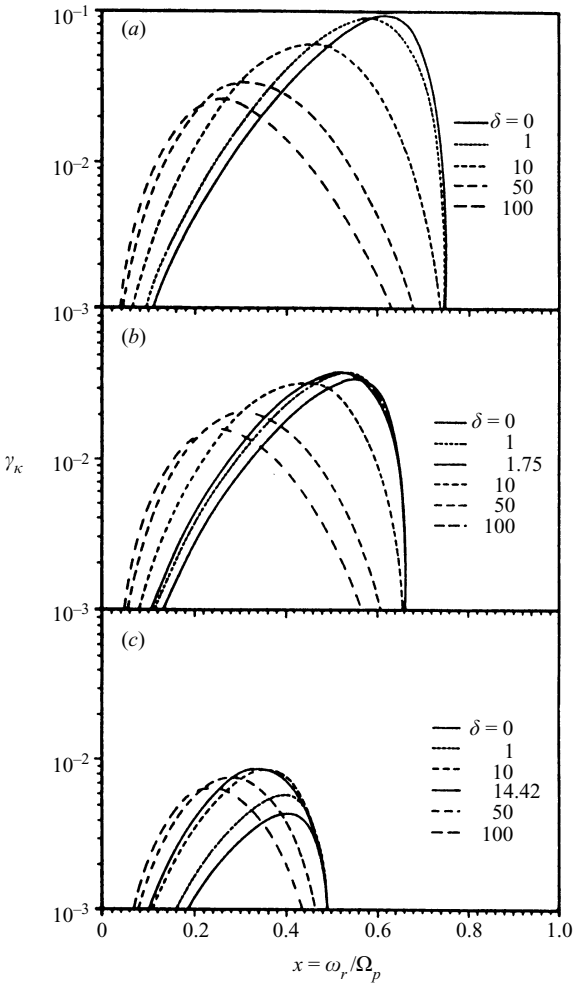


Figure 2. Normalized Lorentzian temporal growth rate versus normalized frequency, for $\beta_{\|p} = 0.1$, $\kappa = 2$, several values of δ, and (*a*) $A_p = 3$, (*b*) $A_p = 2$ and (*c*) $A_p = 1$. Note that in (*b*) the optimum cold-proton concentration is $\delta_{\rm op} = 1.75$, and in (*c*) $\delta_{\rm op} = 14.42$.

3.1.3. Maximum convective growth rate. The convective growth rate is studied here in the same way as the temporal growth rate. Thus, if $I(x) = 1$, (12) gives

$$Q = \frac{(1-x)^3}{\beta_{\|p} x^2 (1+\delta)} = \frac{\kappa - \frac{3}{2}}{\kappa - 1}, \tag{19}$$

and the corresponding mode at which $S_{\kappa,\max}$ occurs is given by

$$x_1(\delta = \delta_{\rm op}) = \frac{A_p - 1}{A_p + 1}. \tag{20}$$

This shows that x_1 is identical to the corresponding value in the Maxwellian case (Gomberoff and Neira 1983), and that, for $A_p \leqslant 1$, $S_{\max}$ is always an increasing function of δ.

https://doi.org/10.1017/S0022377898006382 Published online by Cambridge University Press

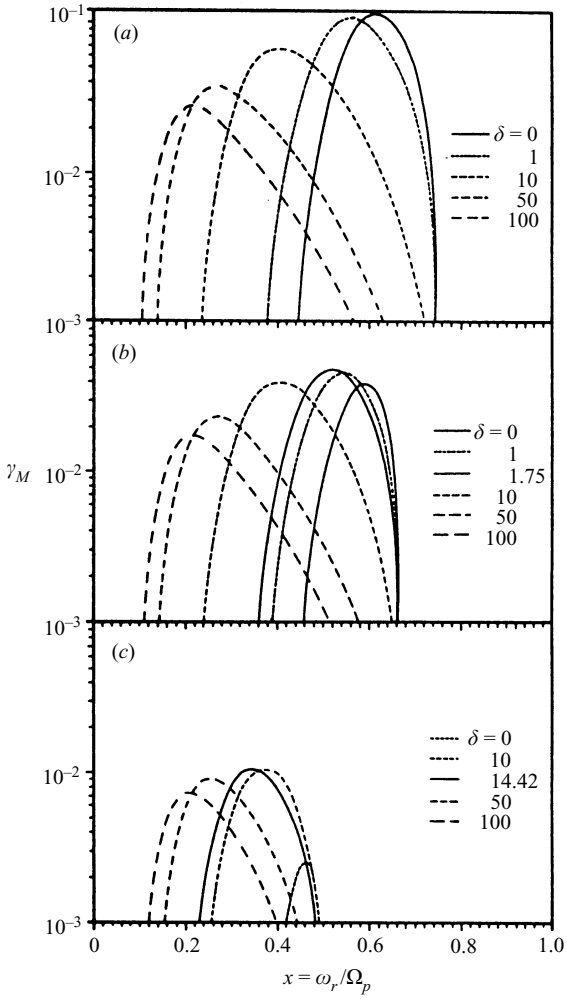


Figure 3. Normalized Maxwellian temporal growth rate versus normalized frequency, for the same parameters as in Fig. 2.

Now, from (19) and (20),

$$\delta_{\rm op} = \left[\frac{\kappa - 1}{\kappa - \frac{3}{2}} \frac{8}{(A_p - 1)^2 (A_p + 1)\beta_{\|p}}\right] - 1. \tag{21}$$

The maximum convective growth rate for $\delta_{\rm op}$ is then

$$S_{\kappa,\max} = \frac{\pi^{1/2}}{2\alpha_{\|p}} \frac{\Gamma(\kappa)[A_p(1 - x_1) - x_1]}{(\kappa - 1)\Gamma(\kappa - \frac{3}{2})} \frac{(\kappa - \frac{3}{2})^{1/2}}{(1 - x_1)^2} \beta_{\|p} \left(1 + \frac{1}{\kappa - 1}\right)^{-\kappa}. \tag{22}$$

The optimum concentration of cold protons and the maximum convective growth rate are then functions of the index κ, and therefore deviations of $\delta_{\rm op}$ and $S_{\kappa,\max}$ should be expected when compared to those in the Maxwellian plasma (Vega *et al.* 1992). As an example, let us consider the typical plasma parameters $\beta_{\|p} = 0.1$ and $A_p = 2$. Also, let us consider values of κ in a range $2 \leqslant \kappa \leqslant 6$, representing the case where the effect of the high-energy particles is more significant. Then the values

https://doi.org/10.1017/S0022377898006382 Published online by Cambridge University Press

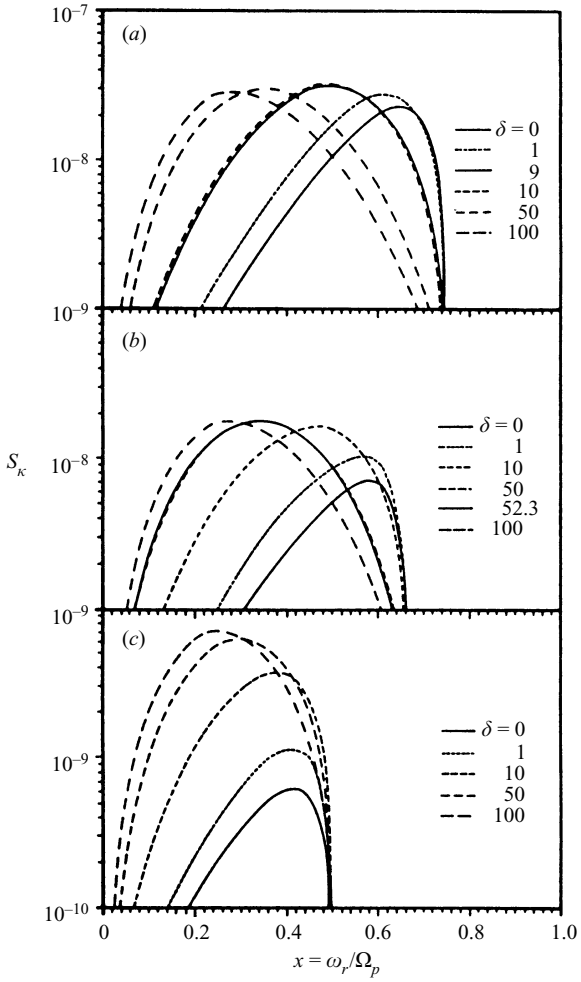


Figure 4. Normalized Lorentzian convective growth rate versus normalized frequency, for $\beta_{\|p} = 0.1$, $\kappa = 2$, several values of δ, and (*a*) $A_p = 3$, (*b*) $A_p = 2$; and (*c*) $A_p = 1$. Note that $\delta_{\rm op} = 9$ in (*a*), and $\delta_{\rm op} = 52.3$ in (*b*).

of $\delta_{\rm op}$ for a Lorentzian plasma are larger than those for a Maxwellian plasma; this difference goes from 100% to 10% as κ moves from 2 to 6.

In order to study whether the deviations predicted above are significant, the convective growth rate S_κ is plotted in Fig. 4 as a function of x, for the same parameters used for the temporal growth rate. In Fig. 4(*a*), $A_p = 3$; it follows from (20), that $x_1 = 0.5$ and $\delta_{\rm op} = 9$, so that $S_{\kappa,\max}(\delta)$ increases until $\delta = \delta_{\rm op}$, to decrease thereafter. In this case, the variation of $S_{\kappa,\max}(\delta)$ is very small. For smaller values of A_p, e.g. $A_p = 2$, from (21), $\delta_{\rm op} = 25.6$; and, from (20), $x_1 = \frac{1}{3}$. As illustrated in Fig. 4(*b*), $S_{\kappa,\max}$ increases significantly until $\delta = \delta_{\rm op}$, to decrease very slowly thereafter.

Let us now consider that A_p is further reduced to 1. From (20), the value of $S_{\kappa,\max}$ corresponding to $\delta = \delta_{\rm op}$ occurs at $x_1 = 0$, and therefore $S_{\kappa,\max}$ is expected to be a monotonically increasing function of δ. This situation is illustrated in Fig. 4(*c*).

https://doi.org/10.1017/S0022377898006382 Published online by Cambridge University Press

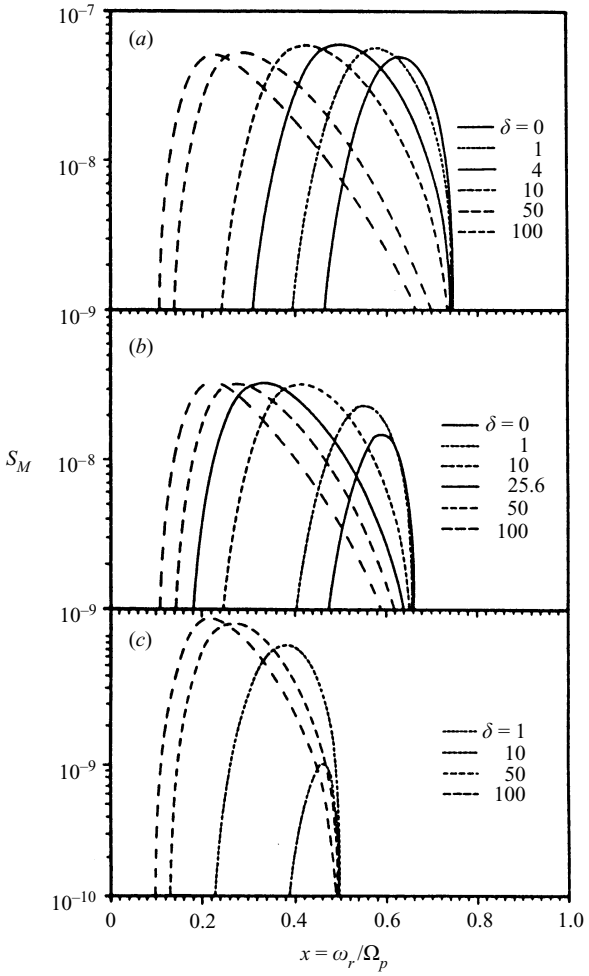


Figure 5. Normalized Maxwellian convective growth rate versus normalized frequency, for the same parameters as in Fig. 4, except that $\delta_{\rm op} = 4$ in (*a*), and $\delta_{\rm op} = 25.6$ in (*b*).

To study the deviations predicted earlier with respect to Maxwellian plasmas, the Maxwellian convective growth rate S_M is plotted in Fig. 5 as a function of x; the same parameters as in Fig. 4 have been considered here. A comparison between these figures shows a similar behaviour of $S_{\max}$. Thus, for $A_p = 3$ and 2, $S_{M,\max}$ increases until $\delta = \delta_{\rm op}$, and decreases slowly thereafter. For $A_p \leqslant 1$, $S_{M,\max}$ will be a monotonically increasing function of δ. Nevertheless, the instability spectrum for a Lorentzian plasma is broader than that for a Maxwellian plasma. This situation was pointed out by Xue *et al.* (1993), using the exact dispersion relation. Even though a decrease in the value of A_p leads to a decrease in $S_{\max}$ for both kinds of plasmas, as was expected from (12) and from the Maxwellian case (Gomberoff and Vega 1989), for $A_p \geqslant 2$, $S_{M,\max}$ is larger than $S_{\kappa,\max}$ for any value of δ. But for smaller values of A_p, $S_{M,\max}$ can become larger than $S_{\kappa,\max}$ only for some values of δ. This situation is shown in Fig. 4(*c*), where $A_p = 1$. For $\delta = 0$, $S_{\kappa,\max}$ is about one order of magnitude larger than $S_{M,\max}$. For $\delta = 1$, $S_{\kappa,\max}$ is of the same order as $S_{M,\max}$. Now, if $\delta = 10$ then $S_{M,\max}$ is larger than $S_{\kappa,\max}$. If δ is increased further

https://doi.org/10.1017/S0022377898006382 Published online by Cambridge University Press

then $S_{M,\max}$ is always larger than $S_{\kappa,\max}$. On the other hand, as predicted from (21), the optimum cold-proton concentration $\delta_{\rm op}$ that is necessary to obtain the optimum Lorentzian convective growth rate for $\kappa = 2$, is over 100% larger than the value in a Maxwellian plasma. Thus, for $A_p = 3$, a value $\delta_{\rm op} = 9$ is necessary to obtain the optimum value of $S_{\kappa,\max}$. But a value of only $\delta_{\rm op} = 4$ is necessary to obtain the optimum value of $S_{M,\max}$. A similar situation occurs for $A_p = 2$.

According to the above considerations, $S_{\kappa,\max}$ can be larger than, equal to or smaller than $S_{M,\max}$, depending on the values of A_p and δ, for fixed values of $\beta_{\|p}$ and κ. Moreover, the optimum value of the maximum convective growth rate is easier to reach in a Maxwellian plasma than in a Lorentzian plasma.

3.1.4. Growth rate as a function of the spectral index κ. The deviations of the growth rate from the Maxwellian case for different values of the spectral index κ are studied in this section. As pointed out earlier, smaller values of κ give a larger proportion of high-energy particles. This may lead us to think that smaller values of κ imply a larger deviation of the growth rate from the value in a Maxwellian plasma. However, from (12) and (13), the growth rates as functions of κ depend significantly on other plasma parameters, such as A_p, δ and $\beta_{\|p}$.

Our study will consider $\beta_{\|p} = 0.1$ as a fixed value. The effects of the variation in $\beta_{\|p}$ were studied by Gomberoff and Rogan (1988) in Maxwellian plasmas and by Xue *et al.* (1993) in Lorentzian plasmas for $\delta = 0$. Therefore the behaviour of the growth rates with varying values of κ, thermal anisotropy and concentration of cold protons is studied here. In order to ensure good results for large values of A_p, let us consider expressions for the growth rates including thermal effects of the energetic protons. Gomberoff and Vega (1989) obtained this aproximation for Maxwellian plasmas; one effect of their corrected approach is a reduction in the growth rates.

The temporal growth rate is plotted in Fig. 6 as a function of x for $\delta = 0$, and $\kappa = 2, 4, 6$ and ∞. Each part corresponds to a given value of A_p. In Fig. 6(a), $A_p = 1$, corresponding to $x_m = 0.5$. It is possible to see that the maximum Lorentzian temporal growth rate for $\kappa = 2$ is significantly higher than in a Maxwellian plasma ($\kappa \to \infty$); that is, for the largest proportion of high-energy particles. An enhancement in the range of instability is observed. Moreover, a decrease in the value of κ, that is, an enhancement of the high-energy population, shifts the maximum growth rate towards lower frequencies.

As mentioned earlier, the thermal anisotropy is generally not a constant in space plasmas. To investigate the effect of its variation, Fig. 6(b) considers $A_p = 1.5$, for the same parameters as in Fig. 6(a). As predicted from (11), an increase in the values of A_p implies that the marginal mode shifts towards higher frequencies, producing an increase in the growth rate; but this enhancement is more effective for larger values of the index κ. Thus, for $A_p = 1.5$, the maximum growth rate $\gamma_{\kappa,\max}$ increases between $\kappa = \infty$ and $\kappa = 4$, and decreases thereafter until $\kappa = 2$. Now, if $A_p = 3$ (Fig. 6c) then $x_m = 0.75$, and a significant increase in the maximum temporal growth rate is verified. The fact that this enhancement is more effective for larger values of κ implies, for a fixed value of A_p, that a decrease in the value of the index κ leads to a decrease in the maximum temporal growth rate, and that the mode at which $\gamma_{\kappa,\max}$ occurs is approximately the same for all values of κ.

Consequently, for $\delta = 0$ fixed, a decrease in the value of κ always produces an enhancement in the instability spectrum and, depending on the value of A_p, the

https://doi.org/10.1017/S0022377898006382 Published online by Cambridge University Press

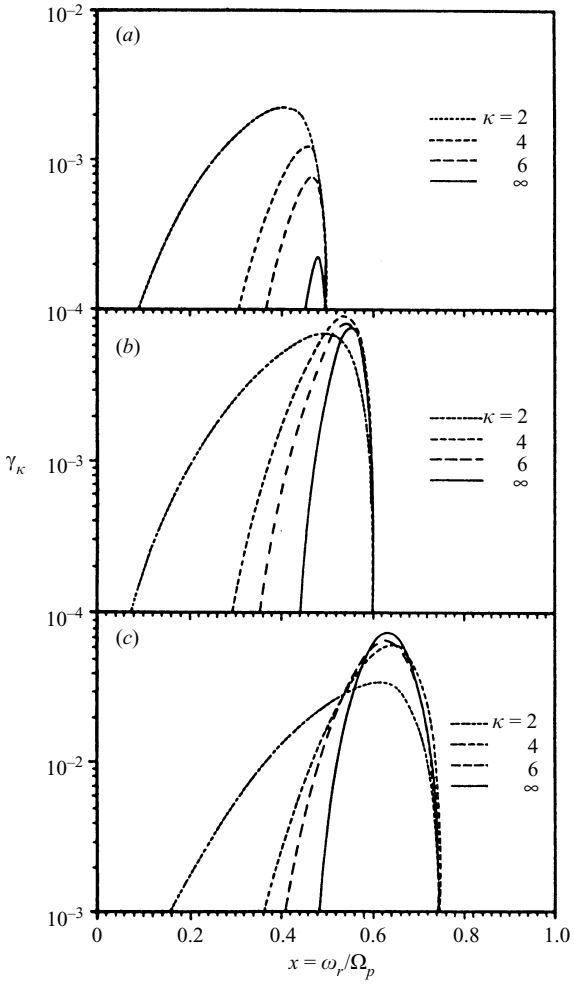


Figure 6. Normalized Lorentzian temporal growth rate versus normalized frequency, for $\beta_{\|p} = 0.1$, $\delta = 0$, several values of κ, and (*a*) $A_p = 1$; (*b*) $A_p = 1.5$ and (*c*) $A_p = 3$.

maximum temporal growth rate can always increase, or increase until $\kappa = \kappa_{\rm op}$ and then decrease, or always decrease.

In order to study the effect of the cold-proton population on the influence of the high-energy tail on EPCWs, Fig. 7 shows γ_κ as a function of κ for different values of δ. By considering $\delta = 0.8$ and $A_p = 0.8$, Fig. 7(*a*) shows that γ_κ exhibits a large increase when κ decreases. This behaviour is similar to that shown in Fig. 6(*a*), where $\delta = 0$ and $A_p = 1$. By now considering $\delta = 1.5$ and $A_p = 1$ (Fig. 7*b*), a significant increase in the value of γ_κ is obtained; but this increase is more effective for larger values of κ. The latter implies that $\gamma_{\kappa,\max}$ increases as κ decreases, until κ reaches a certain optimum value, to decrease thereafter. It is possible to see again that the behaviour shown in Fig. 6(*b*), where $\delta = 0$ and $A_p = 1.5$, has been reproduced. Figure 7(*c*) shows the results for a larger value of the cold-proton concentration, namely, $\delta = 50$ and $A_p = 1$. As can be seen from comparing it with Fig. 7(*b*), this situation leads to an increase in the value of $\gamma_{\kappa,\max}$ and in the

https://doi.org/10.1017/S0022377898006382 Published online by Cambridge University Press

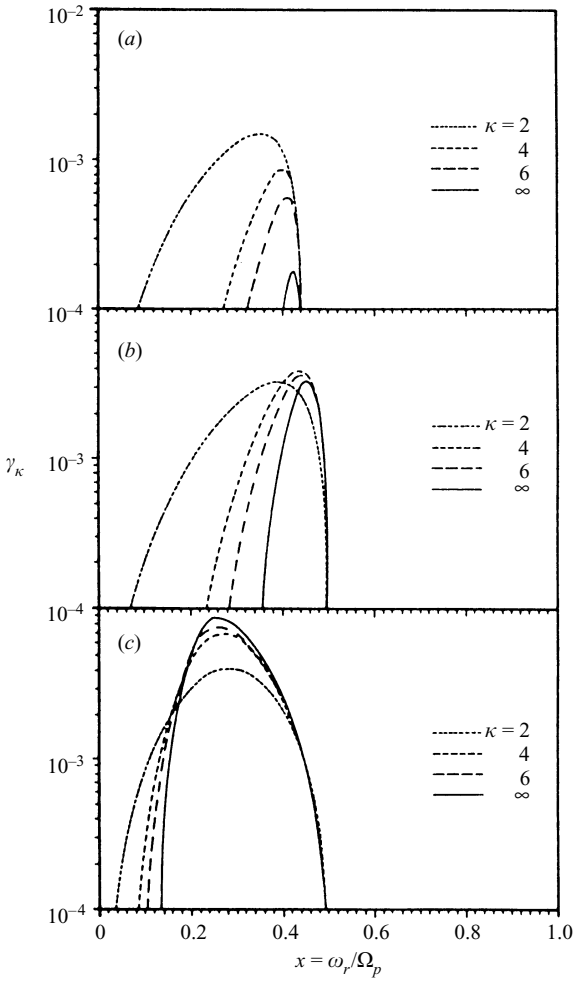


Figure 7. As Fig. 6, but for (*a*) $A_p = 0.8$ and $\delta = 0.8$, (*b*) $A_p = 1$ and $\delta = 1.5$, and (*c*) $A_p = 1$ and $\delta = 50$.

frequency range of the unstable spectrum. In other words, decreasing values of the spectral index κ lead to a decrease in $\gamma_{\kappa,\max}$ and to an enhancement in the unstable spectrum.

The same procedure as in Figs 6 and 7 has been followed in Figs 8 and 9, but now for the convective growth rate. It is possible to see that the behaviour of S_κ is very similar to that for the temporal growth rate. Consequently, when studying the effect of the high-energy tail of the distribution on wave growth, one must take into account the fact that δ and A_p are generally variable during the generation and propagation of EPCWs. This implies that when the number of high-energy particles increases, that is, when κ decreases, the maximum Lorentzian growth rate can always increase, or increase until κ reaches a certain value and then decrease, or always decrease. Thus, depending on the values of A_p and δ, growth rates for plasmas modelled by a kappa distribution could be larger than, or approximately equal to, or smaller than the value in a plasma modelled by a Maxwellian distribution.

https://doi.org/10.1017/S0022377898006382 Published online by Cambridge University Press

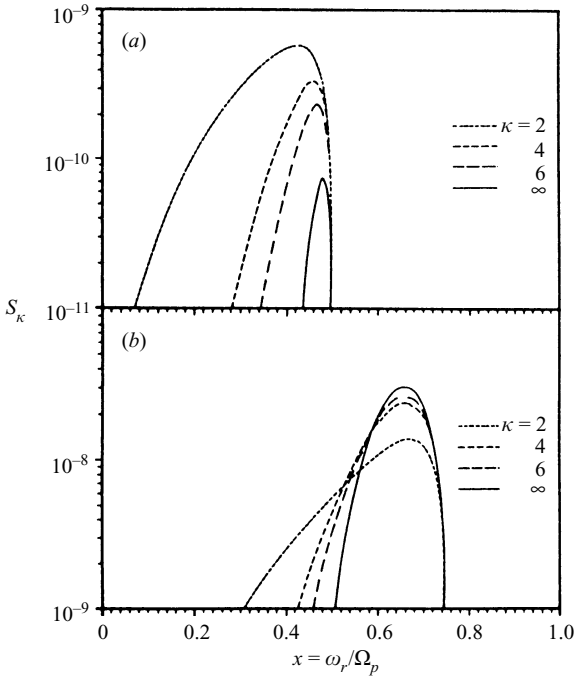


Figure 8. Normalized Lorentzian convective growth rate versus normalized frequency, for $\beta_{\|p} = 0.1$, $\delta = 0$, several values of κ, and (*a*) $A_p = 1$ and (*b*) $A_p = 3$.

4. Summary and conclusions

An analytical and parametric study of the L mode in electromagnetic ion-cyclotron waves in a multi-ion plasma modelled by a bi-Lorentzian distribution function has been presented here. General analytical expressions for the wavenumber and for both the temporal and convective growth rates for a multicomponent plasma have been obtained. A comparison with those in a bi-Maxwellian plasma shows that the wavenumber equations are similar. The characteristics of the unstable spectrum are found to be independent of the high-energy particles.

With respect to the amplification process, the effect of the high-energy tail of the distribution function depends strongly on the characteristic plasma parameters. This approach, called the semicold approximation, applied to a plasma composed of hot protons and electrons proves to be a very good approximation for $\beta_{\|p} < 1$, a situation that is common in space plasmas. The fact that space plasmas are multicomponent systems, and the need to study the influence of other components, led us to consider a second cold-proton component.

The behaviour of the maximum growth rate as a function of the cold-proton concentration for different values of the thermal anisotropy of the hot protons has been studied for the greatest number of high-energy particles, i.e. $\kappa = 2$. The instability range was found to be much broader than that in a Maxwellian plasma. As in the case of Maxwellian plasmas, the maximum Lorentzian growth rates decrease when A_p decreases. These results were also obtained by Xue *et al.* (1996) by solving the exact relations numerically. However, this analytical approach shows that the maximum growth rates as functions of cold-proton concentration can always decrease, or increase until δ reaches a certain optimum value and then decrease, or always

https://doi.org/10.1017/S0022377898006382 Published online by Cambridge University Press

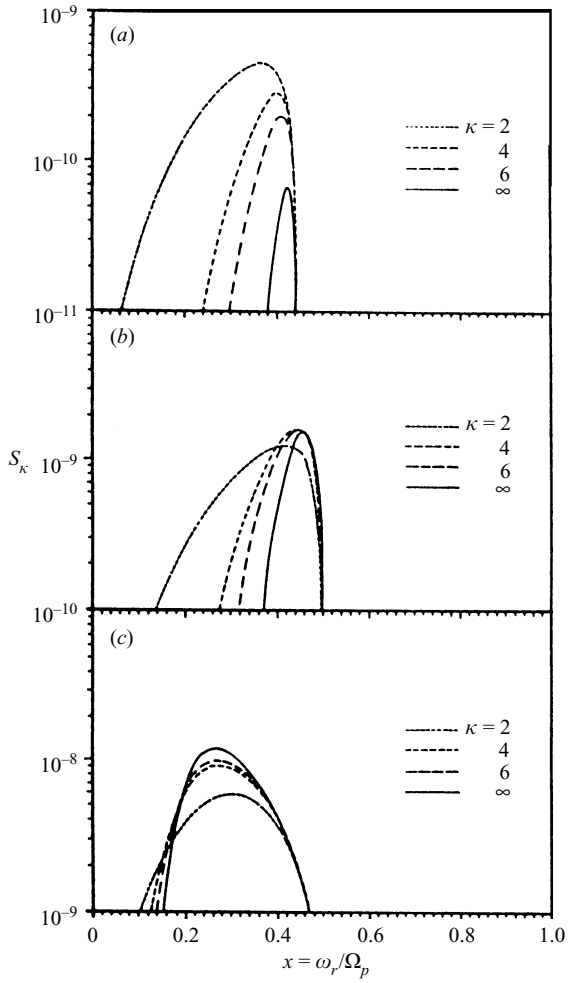


Figure 9. As in Fig. 8, but for (*a*) $A_p = 0.8$ and $\delta = 0.8$, (*b*) $A_p = 1$ and $\delta = 1.5$ and (*c*) $A_p = 1$ and $\delta = 50$.

increase, depending on the value of A_p. The mode at which the maximum temporal growth rate occurs, as well as the corresponding optimum cold-proton concentration, are given by the same expressions as obtained in a Maxwellian plasma. Despite the fact that the mode at which the maximum convective growth rate occurs is given by the same expression as in a Maxwellian plasma, the expression for the optimum cold-proton concentration depends significantly on the spectral index κ. As a result, in the range of values of κ for which the hot components of the space plasmas are significant, i.e. $2 \leqslant \kappa \leqslant 6$, the differences in the optimum growth rates go from 100% to 10% larger than those in a Maxwellian case, as κ moves from 2 to 6. This means that the optimum amplification through the injection of a cold-proton population is more difficult to reach in a Lorentzian plasma than in a Maxwellian plasma.

Finally, it has been shown that the influence of the high-energy tail on the generation and amplification of electromagnetic proton-cyclotron waves depends on the values of the thermal anisotropy and on the cold-proton population. That is,

https://doi.org/10.1017/S0022377898006382 Published online by Cambridge University Press

temporal and convective growth rates can be larger than, equal to or smaller than those for a Maxwellian plasma, depending on the anisotropy of the hot-proton distribution and on the cold-proton concentration. In other words, the maximum Lorentzian growth rates as functions of κ can always decrease, or increase until κ reaches some optimum value $\kappa_{\rm op}$ and then decrease, or always increase, depending on both the thermal anisotropy and the cold-proton concentration.

Consequently, a great variety of multicomponent space plasmas can be studied using the analytical semicold approximation. When studying EPCWs, this approach leads to better understanding of the interplay between the characteristic parameters of the different plasma components. As an important final comment, it must be said that the complexity of the dynamics of space plasmas requires a detailed study of the role played by each ion component in the electromagnetic ion-cyclotron waves.

References

Anderson, B. J., Erlandson, R. E. and Zanetti, L. J. 1992*a* A statistial study of Pc 1-2 magnetic pulsations in the equatorial magnetosphere, 1. Equatorial occurrence distributions. *J. Geophys. Res.* **97**, 3075–3088.

Anderson, B. J., Erlandson, R. E. and Zanetti, L. J. 1992*b* A statistical study of Pc 1-2 magnetic pulsations in the equatorial magnetosphere, 2. Wave properties. *J. Geophys. Res.* **97**, 3089–3101.

Christon, S. P., Williams, D. J., Mitchell, D. G., Frank, L. A. and Huang, C. Y. 1989 Spectral characteristics of plasma sheet ion and electron populations during undisturbed geomagnetic conditions. *J. Geophys. Res.* **94**, 13 409–13 424.

Gendrin, R., Ashour-Abdalla, M., Omura, Y. and Quest, K. 1984 Linear analysis of ion cyclotron interaction in a multicomponent plasma. *J. Geophys. Res.* **89**, 9119–9124.

Gomberoff, L. and Cuperman, S. 1982 Combined effect of cold H^+ and He^+ ions on the proton cyclotron electromagnetic instability. *J. Geophys. Res.* **87**, 95–100.

Gomberoff, L. and Neira, R. 1983 Convective growth rate of ion cyclotron waves in a H^+–He^+ and H^+–He^+–O^+ plasma. *J. Geophys. Res.* **88**, 2170–2174.

Gomberoff, L. and Rogan, J. 1988 Comparative study of the effect of cold ions and thermal anisotropy on the convective electromagnetic proton cyclotron instability. *Planet. Space Sci.* **36**, 207–212.

Gomberoff, L. and Vega, P. 1987 Effect of He^+ ion temperature and thermal anisotropy on the proton cyclotron instability at the geosynchronous region of GEOS-2. *J. Geophys. Res.* **92**, 7728–7732.

Gomberoff, L. and Vega, P. 1989 Electromagnetic ion cyclotron waves with frequency below the proton gyrofrequency in large β multicomponent plasmas. *Plasma Phys. Contr. Fusion* **31**, 629–641.

Isenberg, P. A. and Hollweg, J. V. 1983 On the preferential acceleration and heating of solar wind heavy ions. *J. Geophys. Res.* **88**, 3923–3935.

Ishida, J., Kokubun, S. and McPherron, R. L. 1987 Substorm effect on spectral structures of Pc1 waves at synchronous orbit. *J. Geophys. Res.* **92**, 143–158.

Lui, A. T. and Krimigis, S. M. 1983 Energetic ion beam in the Earth's magnetotail lobe *Geophys. Res. Lett.* **10**, 13–16.

Marsch, E., Goertz, C.K. and Richter, K. 1982 Wave heating and acceleration of solar wind ions by cyclotron resonances. *J. Geophys. Res.* **87**, 5030–5044.

Mauk, B. H., Keath, E. P., Kane, M., Krimigis, S. M., Cheng, A. F., Acuña, M. H., Armstrong, T. B. and Ness N. F. 1991 The magnetosphere of Neptune: hot plasmas and energetic particles. *J. Geophys. Res.* **96**, 19 061–19 084.

Ogilvie, K. W., Geiss, J., Gloeckler, G., Berdichevsky, D. and Wilken, B. 1993 High-velocity tails on the velocity distribution of solar wind ions. *J. Geophys. Res.* **98**, 3605–3611.

https://doi.org/10.1017/S0022377898006382 Published online by Cambridge University Press

Roux, A., Perraut, S., Rauch, J. L., De Villedary, C., Kremser, G., Korth, A. and Young, D. T. 1982 Wave–particle interactions near Ω_{He^+} observed on GEOS 1 and 2. 2. Generation of ion cyclotron waves and heating of He^+ ions. *J. Geophys. Res.* **87**, 8174–8190.

Summers, D. and Thorne, R. M. 1991 The modified plasma dispersion function. *Phys. Fluids* **B3**, 1835–1847.

Summers, D. and Thorne, R. M. 1992 A new tool for analyzing microinstabilities in space plasmas modelled by a generalized Lorentzian (kappa) distribution. *J. Geophys. Res.* **97**, 16 827–16 832.

Vasyliunas, V. M. 1968 A survey of low-energy electrons in the evening sector of the magnetosphere with OGO 1 and OGO 3. *J. Geophys. Res.* **73**, 2839–2884.

Vega P., Fernández, J. and Gomberoff, L. 1992 Role of cold H^+ and He^+ ions and thermal anisotropy in the electromagnetic proton cyclotron instability. *Geofis. Inter.* **31**, 131–134.

Williams, D. J., Mitchell, D. G. and Christon, S. P. 1988 Implications of large flow velocity signatures in nearly isotropic ion distributions. *Geophys. Res. Lett.* **15**, 303–306.

Xue, S., Thorne, R. M. and Summers, D. 1993 Electromagnetic ion-cyclotron instability in space plasmas. *J. Geophys. Res.* **98**, 17 475–17 484.

Xue, S., Thorne, R. M. and Summers, D. 1996 Parametric study of electromagnetic ion cyclotron instability in the Earth's magnetosphere. *J. Geophys. Res.* **101**, 15 467–15 474.

Young, D. T., Perraut, S., Roux, A., De Villedary, C., Gendrin, R., Korth, A., Kremser, G. and Jones, D. 1981 Wave particle interaction near Ω_{He^+} observed on GEOS 1 and 2. Propagation of ion cyclotron waves in He^+- rich plasma. *J. Geophys. Res.* **86**, 6755–6772.

https://doi.org/10.1017/S0022377898006382 Published online by Cambridge University Press